BJRS

BRAZILIAN JOURNAL
OF
RADIATION SCIENCES
10-03B (2022) 01-11

Evaluation of mass attenuation coefficient of concrete sample for different traits

Bastos[a] L.F., Teixeira[a] T.P., Gama Filho[b] H., Calixto[c] S., Gonçalves[c] M., dos Anjos[b] M.J., Lopes[a] R.T., Oliveira[a] D.F.

[a]*Nuclear Instrumentation Laboratory/PENCOPPE/UFRJ, Rio de Janeiro, RJ, Brazil*

[b]*Electronic Instrumentation and Analytical Techniques Laboratory/IF/UERJ, Rio de Janeiro, RJ, Brazil*

[c]*Engineering and Technology Institute/Geraldo di Biase University, Volta Redonda, RJ, Brazil*

luanfbastos@gmail.com

ABSTRACT

Concrete is widely used in the world and is the main material for civil construction. Due to its properties, it has different uses such as structural, filling and shielding. The aim of this work is to compare experimental and theoretical mass attenuation coefficient for concrete with different traits and determine the one with the best performance. For this, density, X-ray diffraction, mass attenuation coefficient (experimental with a Cs137 source, simulated by MCNP and theoretical determined with XCOM platform) and compressive strength were determined for three different traits of cement mortar (standardized sand, conventional sand and artificial sand). The X-ray diffraction showed more compounds for artificial sand's samples. Density showed no significant variation. The samples showed a good agreement for experimental, simulated and theoretical mass attenuation coefficient. Standardized sand's samples had the best performance for mechanical test, with a compressive strength 47.4% higher than artificial sand's samples and 38.2% higher than conventional sand's samples. It is possible to conclude that, since mass attenuation coefficient showed no significant difference, standardized sand's samples is more indicated to be used for shielding than the others.

Keywords: **cement mortar, MCNP, mass attenuation coefficient, X-ray diffraction, XCOM.**

ISSN: 2319-0612
DOI: https://doi.org/10.15392/2319-0612.2022.1915
Submitted: 2022-01-30
Accepted: 2022-08-01

1. INTRODUCTION

Concrete is a composite material that consists essentially of a binding medium within which are embedded particles or fragments of aggregate [1] and is widely used in different ways such as structural, filling and shielding. The use as shielding is important in nuclear installations and radiation therapy rooms due to the attenuation properties of the beams from nuclear reactions and to protect people from radiation.

Gamma ray photon interacts with matter and three phenomena can be observed: photoelectric effect (τ), Compton scattering (σ) and production of pairs (κ). Each of the interaction processes removes the gamma ray photon from the beam either by absorption or by scattering away from the detector direction and can be characterized by a fixed probability of occurrence per unit path length in the absorber thickness. The sum of these probabilities is simply the probability per unit path length that gamma ray photon is removed from the beam, as in equation 1, and is called as linear attenuation coefficient (μ) [2].

$$\mu = \tau + \sigma + \kappa \tag{1}$$

The mass thickness of the absorber determines degree of attenuation. In this way, the thickness of absorbers used in radiation measurements is therefore often measured in mass thickness rather than physical thickness, because it is a more fundamental physical quantity. Units of mass thickness have historically been mg/cm^2 [2] in equation 2. This relationship allows us to infer that the higher the density in the medium, the more effective the attenuation of gamma radiation will be.

$$\frac{I}{I_0} = e^{-\left(\mu/\rho\right)\rho x} \tag{2}$$

The gamma transmission technique is a method used to determining the attenuation coefficient of different types of materials and elements and is based in the Beer-Lambert's law [2]. This technique employs a monoenergetic gamma ray source and a high-efficiency detector. Both devices

are placed on the same horizontal plane and positioned at 180 degrees from each other. The transmitted intensities are recorded by the electronic components associated with the detector and can be displayed as an energy spectrum. This technique is widely used for calculating the attenuation coefficient of concrete samples [3-7]. The aim of this work is to compare experimental results with theoretical mass attenuation coefficient, determined by XCOM, and simulated mass attenuation coefficient, determined by MCNP, for concrete with different traits.

2. MATERIALS AND METHODS

The samples used in this study are sixty-three 100 mm x 50 mm (H x d) plugs, as determined in NBR 7215 standard [8], divided in three traits that are listed in table 1. The IPT samples were prepared with standard sand as determined in NBR 7211 standard [9], the CON samples were prepared using conventional sand that can be bought in any hardware store and the ART samples were prepared with artificial sand (gravel that can be classified as fine aggregate). It was used a water cementing rate of 0.48 and 40 MPa cement.

Density was determined by the displacement technique and is also presented in table 1. A glass beaker was filled up with distilled water and its density was determined by using an aluminum cylinder with known weight and volume by equation 3. After calculating the water density, the equation 4 was used to calculate the mortar density. In equation 3, M_{Al} is the aluminum cylinder weight in container filled up with water without touching its bottom and V_{Al} is the aluminum cylinder volume. In equation 4, M_{air} is mortar mass in air, M_{water} is mortar mass in water container without touching its bottom and ρ_{H2O} is the water density. Mortar samples were wrapped in plastic film to avoid penetration of water.

$$\rho_{H_2O} = \frac{M_{Al}}{V_{Al}} \tag{3}$$

$$\rho_{conc} = \frac{M_{air}}{M_{water}} \rho_{H_2O} \tag{4}$$

Table 1: Quantity of elements used in mortar samples.

Samples	Cement (g)	Standard Sand (g)	Conventional Sand (g)	Artificial Sand (g)	Density (g/cm^3)
IPT	642	1,872	-	-	2.076
CON	642	-	1,872	-	2.059
ART	642	-	-	1,872	2.120

To determine the linear attenuation coefficient for the 662 keV energy peak, a gamma-ray transmission system was used, consisting of a 1.96 GBq Cs^{137} radiation source, collimated with a cylindrical lead collimator of 5 mm in diameter and a 2 x 2 in NaI(Tl) scintillation detector, also collimated with a cylindrical collimator of 5 mm in diameter. The signals from the detector were processed by standard gamma ray electronics, consisting of a pre-amplifier, an amplifier and a multichannel analyzer for acquiring the energy spectrum.

The number of counts reaching the detector with and without the samples was recorded for the same counting live time of 300 s and the distance between the radiation source and the detector was 15 cm.

The mass attenuation coefficient (μ/ρ) was calculated following the Beer-Lambert's Law for a monoenergetic radiation beam, as shown in equation 5, I_0 is the intensity recorded without the sample, I is the intensity recorded with sample, t is the thickness of sample and ρ is the sample density. Figure 1 shows the experimental setup.

$$\mu/\rho = \frac{\ln(I_0) - \ln(I)}{t \times \rho} \tag{5}$$

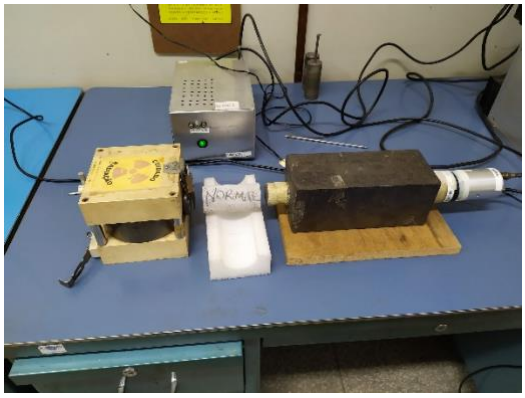

Figure 1: *Experimental setup to determine attenuation coefficient.*
Source: from the author.

To determine the composition of each trait, X-ray diffraction was used. The samples were passed through a nylon mesh sieve with a 50 μm opening and the analysis was performed by a commercial benchtop equipment D2 Phaser from BRUKER. A voltage of 30 kV, a current of 10 mA, filter kβ of Ni, with a measurement time of 0.5 s, with an initial angle of 5º and a final angle of 90º at a step of 0.01º used for the scan. With the elements defined, they were used into the XCOM platform to identify the attenuation coefficient. They were also inserted into an MCNP code that reproduced the system setup so that data could be validated. Figure2 shows the geometry used in MCNP simulation setup.

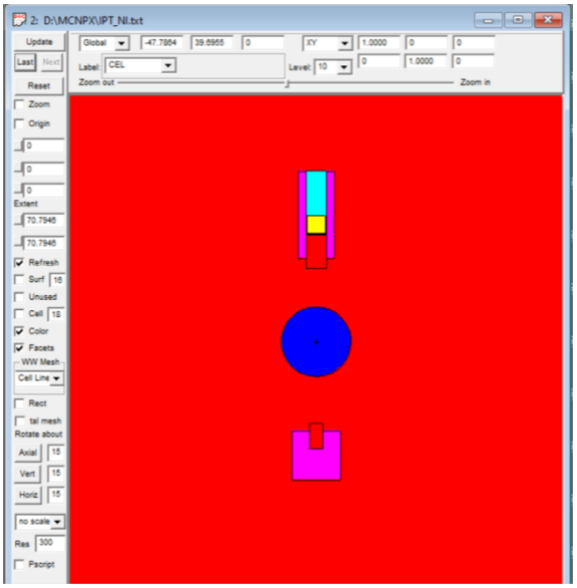

Figure 2: Geometry setup used in MCNP.
Source: from the author.

The mechanical test was performed using Contenco's hydraulic press. The maximum load capacity is 100 T and the maximum sample height is 145 mm. The mechanical test was performed when the samples reached 76 days. The test was performed for all samples and an average for compressive strength was determined for irradiations samples.

NBR 7215 [8] determines how the mechanical test has to be done. Loading shall be carried out at a speed of 0.25 ± 0.05 MPa/s and at a constant load speed throughout the test. The calculation of average resistance is performed through the arithmetic mean of each group.

3. RESULTS AND DISCUSSION

Table 2 shows each compound identified through X-ray diffraction. It is possible to notice that ART samples presented more compounds in its structure than the others.

For IPT and CON samples, quartz is the most abundant compound as expected, since sand was used in their traits, but for ART samples is albite. Portlandite, calcite, vaterite are presented in all as expected, since they are compounds found in mortar samples. Another compound normally found in mortar samples is albite, but it is not present in CON samples.

These results were the input for MCNP code and XCOM platform to determine mass attenuation coefficient for 662 kV energy.

Table 2: Elemental composition.

Compound	Chemical formula	ART (%)	IPT (%)	CON (%)
Quartz	O2Si	28.0	67.5	53.1
Calcite	CCaO3	3.1	6.9	12.9
Albite	AlNaO8Si3	28.3	7.9	-
Vaterite	CCaO3	6.1	10.4	12.0
Microcline	AlK0.89Na0.11O8Si3	23.4	-	21.1
Annite	Al3.156Fe1.624K0.928O12Si2.32	4.4	-	-
Organic Compound	C10H7NO3	3.7	-	-
Bassanite	CaHO4.5S	0.8	-	-
Anhydrite	CaO4S	1.9	-	-
Portlandite	CaH2O2	0.3	2.9	0.8
Berlinite	AlO4P	-	4.3	-

Table 3 compares the mass attenuation coefficient for the energy of 662 keV of experimental, XCOM platform and MCNP code and the absolute error and the relative error. Although the samples had different fine aggregates, they presented a similar value for the mass attenuation coefficient for 662 kV energy. The proximity of mass attenuation coefficients was expected when the density, which was presented in table 1, is analyzed. The experimental mass attenuation coefficient was determined by equation 5.

Calculation of errors considered result found on XCOM platform as a theoretical reference. The relative error found for the experimental value of ART is 5.3%, but it is still considered a good parameter. For absolute error, the value found for ART experimental samples was just 0.41% and it also is a good parameter. In this way, this work presents a good agreement between experimental setup, XCOM (theoretical) and MCNP (simulated). Experimental results were always higher than the results determined by XCOM, but the values are in good agreement, since relative error does not

show a variation greater than 5.3%. A better agreement is found between the values determined by XCOM and those simulated by MCNP, since relative error does not present a variation greater than 2.21%.

Table 3: Mass Attenuation Coefficient for experimental setup, XCOM and MCNP.

Samples	Mass Attenuation Coefficient ($x10^{-2}$ cm2/g)			Absolute Error		Relative Error	
	XCOM	Experimental	MCNP	Experimental	MCNP	Experimental	MCNP
IPT	7.73	8.00	7.65	-0.27%	0.08%	-3.5%	1.03%
CON	7.72	8.06	7.74	-0.34%	-0.02%	-4.4%	-0.26%
ART	7.70	8.11	7.53	-0.41%	0.17%	-5.3%	2.21%

Results for compressive strength are shown in figure 3. The results showed that IPT had the higher compressive strength (63.7 MPa), CON had 39.3 MPa and ART had the lower (33.5 MPa). The difference between IPT and ART was of 30.2 MPa and 24.3 MPa between IPT and CON. The mechanical strength test shows that mortar with standardized sand has a better performance.

As density is related to mechanical strength, it is expected that a denser mixture presents a greater resistance to compressive strength, if the samples had the same preparation and water/cement ratio are respected, as aggregate occupy about 80% of the concrete volume. Besides that, it is important to notice that the aggregate's density is what define the use of cement mortar [10-12]. In this way, it was expected that samples had close values for compressive strength. Higher value for IPT samples demonstrated that standardized sand is more homogeneous than conventional sand and had a better performance than the fine aggregates used in ART samples. When the results for X-ray diffraction is analyzed, it was expected that a different in mechanical properties could be found.

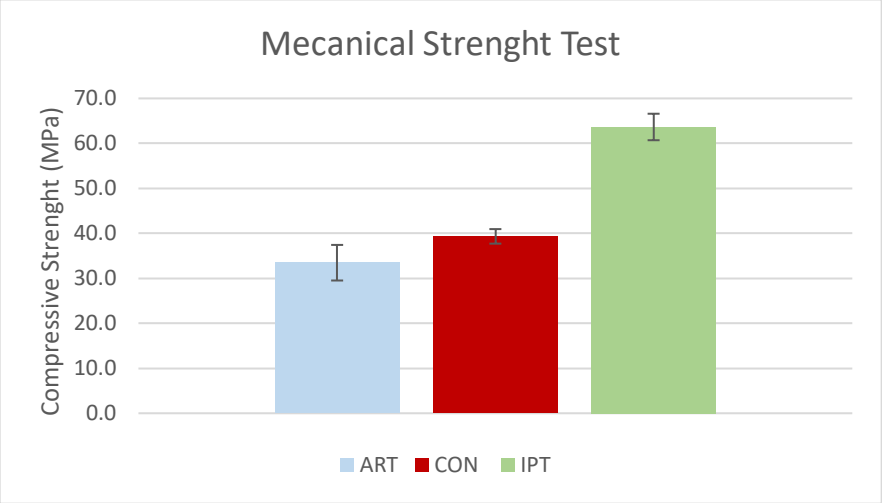

Figure 3: Mechanical strength test results.
Source: from the author.

When mass attenuation coefficient and mechanical strength test are analyzed together, is possible to notice that IPT samples had better performance than the others.

4. CONCLUSION

The mass attenuation coefficient showed good agreement for the experimental setup and theoretical values. The three different traits didn't show any significant difference in attenuation of 662 kV photon.

The X-ray diffraction showed a difference in each compound. ART samples presented more chemical elements in its structure, but this did not affect the mass attenuation coefficient and the samples showed close results.

The mechanical test showed very different values for each trait. IPT samples had the best performance, while ART and CON showed closer results. This was not expected, since materials with similar density are expected to present similar values for compressive strength. It is possible to conclude from this result that the artificial sand does not present the same performance as the other sands, because the performance in the mechanical test was the lowest. It is also possible to conclude

that the use of non-standard sand can significantly affect the mechanical strength compared to standardized sand.

The sample with standardize sand is more indicated to be used for shielding than the other traits.

Further studies are needed to indicate to understand how mortar with different fine aggregates works for shielding purpose.

ACKNOWLEDGMENT

This study was financed in part by the Coordenação de Aperfeiçoamento de Pessoal de Nível Superior - Brasil (CAPES) - Finance Code 001. The authors also would like to thank the Conselho Nacional de Desenvolvimento Científico e Tecnológico (CNPq) and Fundação de Amparo à Pesquisa do Estado do Rio de Janeiro (FAPERJ) for their financial support.

REFERENCES

[1] ASTM C125 - **Standard Terminology Relating to Concrete and Concrete Aggregates**, ASTM International, West Conshohocken, PA (2018).

[2] Knoll, G. F., **Radiation Detection and Measurement**, 3rd ed. New York: John Wiley & Sons, 1999.

[3] SALINAS, I.; CONTI, C.; LOPES, R. Effective density and mass attenuation coefficient for building material in Brazil. **Applied Radiation and Isotopes**, v. 64, pp 13-18, 2005.

[4] AKKURT, I.; AKYILDIRIM, H.; MAVI, B.; KILINCARSLAN, S.; BASYIGIT, C. Photon attenuation coefficients of concrete includes barite in different rate.**Annals of Nuclear Energy**, v. 37, pp. 910-914, 2010.

[5] DAMLA, N.; BALTAS, H.; CELIK, A., KIRIS, E., CEVIK, U. Calculation of radiation attenuation coefficients, effective atomic numbers and electron densities for some building materials.**Radiation Protection Dosimetry**, v. 150 (4), pp. 541-549, 2012.

[6] UN, A.; DEMIR, F.Determination of mass attenuation coefficients, effective atomic numbers and effective electron numbers for heavy-weight and normal-weight concretes. **Applied Radiation and Isotopes**, v. 80, pp. 73-77, 2013.

[7] GOKÇE, H. S.; OZTURK, B. C.; ÇAM, N. F.; ANDIÇ-ÇAKIR, O. Gamma-ray attenuation coefficients and transmission thickness of high consistency heavyweight concrete containing mineral admixture. **Cement and Concrete Composites**, v. 92, pp. 56-69, 2018.

[8] NBR 7215 - **Cimento Portland - Determinação da resistência à compressão de corpos de prova cilíndricos**, Associação Brasileira de Normas Técnicas (2019).

[9] NBR 7211 - **Agregados para concreto - Especificação**, Associação Brasileira de Normas Técnicas (2009).

[10] MEHTA, P. K.; MONTEIRO, P. J. M., **Concrete: Microstructure, Properties, and Materials**, 3 ed., California, McGraw-Hill Companies, 2006.

[11] MASLEHUDDIN, M.; SHARIF, A. M.; SHAMEEM, M.; IBRAHIM, M.; BARRY, M. S. Comparison of properties of steel slag and crushed limestone aggregate concretes. **Construction and Building Materials**, v. 17, pp. 105-112, 2003.

[12] TOPÇU, I. B. Properties of heavyweight concrete produced with barite, **Cement and Research**, v.33, pp. 815-822, 2003.